Estuaries Vol. 25, No. 4A, p. 508–518 August 2002

Impact of the Spring 2000 Phytoplankton Bloom in Chesapeake Bay on Optical Properties and Light Penetration in the Rhode River, Maryland

CHARLES L. GALLEGOS* and THOMAS E. JORDAN

Smithsonian Environmental Research Center, P. O. Box 28, Edgewater, Maryland 21037

ABSTRACT: Accelerating eutrophication manifest as increasing frequency and magnitude of phytoplankton blooms threatens living resources in many estuaries. Effects of large blooms can be difficult to document because blooms are often unexpected and do not always coincide with scheduled sampling programs. Here we use continuously monitored salinity distributions and optical properties to study the spring bloom of the red tide dinoflagellate, *Prorocentrum minimum*, in the Rhode River, Maryland, a tributary embayment of upper Chesapeake Bay. Salinity distributions, together with weekly cruise measurements of nutrient concentrations, indicate that the bloom commenced with an influx of nitrate at the mouth due to the arrival of a freshet from the Susquehanna River. Arrival of this freshet at the mouth set up an unstable, inverse salinity gradient within the Rhode River. Continuously monitored absorption and scattering spectra indicated that increases in chlorophyll within the Rhode River initially were due to the influx of chlorophyll that had developed in the main stem of the bay. After the influx, much higher concentrations and steep spatial gradients developed within the Rhode River, subsequent to reduced mixing that accompanied re-establishment of a normal estuarine salinity gradient. We used the monitored absorption and scattering coefficients to determine the effect of the bloom on light attenuation coefficients in the Rhode River. The bloom resulted in a nearly three-fold increase in attenuation coefficient. Attenuation was dominated by chlorophyll in the early stages of the bloom and by detritus after the termination of the bloom. Although the bloom lasted only 20 d, the elevated attenuation coefficients due to the bloom exceeded values that would permit growth of submersed vascular plants for a period of about 45 d.

Introduction

Accelerating eutrophication due to anthropogenic nutrient enrichment threatens ecosystem structure and function at sites along coastlines of every inhabited continent (Richardson and Jorgensen 1996). Effects of eutrophication depend on the length and extent of nutrient overenrichment. Chronic effects include changes in the total standing crop, species composition, and size distribution of phytoplankton, increases in frequency and magnitude of nuisance and harmful algal blooms (Smayda 1990), hypoxia caused by increased loading of organic matter to the bottom, and reduced light penetration and loss of habitat for submersed vascular plants.

Periodic outbreaks of the dinoflagellate *Prorocentrum minimum* have been observed in upper Chesapeake Bay for many years (Tyler and Seliger 1978). Details of the seeding mechanism and time course for development of these blooms have been determined (Tyler and Seliger 1978) as well as physiological adaptations of *Prorocentrum* to prolonged transport under conditions of low light (Harding and Coats 1988). Impacts of specific bloom events can be difficult to determine because they are often unexpected, patchy, ephemeral, and may be gone before researchers can react with sampling efforts.

Automated water quality instruments have been successfully used to monitor aspects of aquatic system metabolism and water quality (Kelly et al. 1974). In situ instruments have the potential to provide uninterrupted coverage of those parameters amenable to automated recording. Recent advances in measurement of optical properties of natural waters has expanded the parameters available for automated monitoring of aquatic systems (Dickey et al. 1998; Chang and Dickey 1999). Optical properties are especially informative because they are determined by 3 parameters: colored dissolved organic matter (CDOM), phytoplankton chlorophyll, and suspended particulate matter (SPM). These three parameters are diagnostic indicators of a wide variety of natural and anthropogenic stressors that impinge on estuaries. Phytoplankton blooms, in particular, have the potential to elevate all three of these parameters. In addition, optical properties of water (in particular the inherent optical properties, which depend only on the concentrations and types of materials present in the water) determine the underwater light

* Corresponding author; tele: 443/482-2240; fax: 443/482-2380; e-mail: gallegos@serc.si.edu.

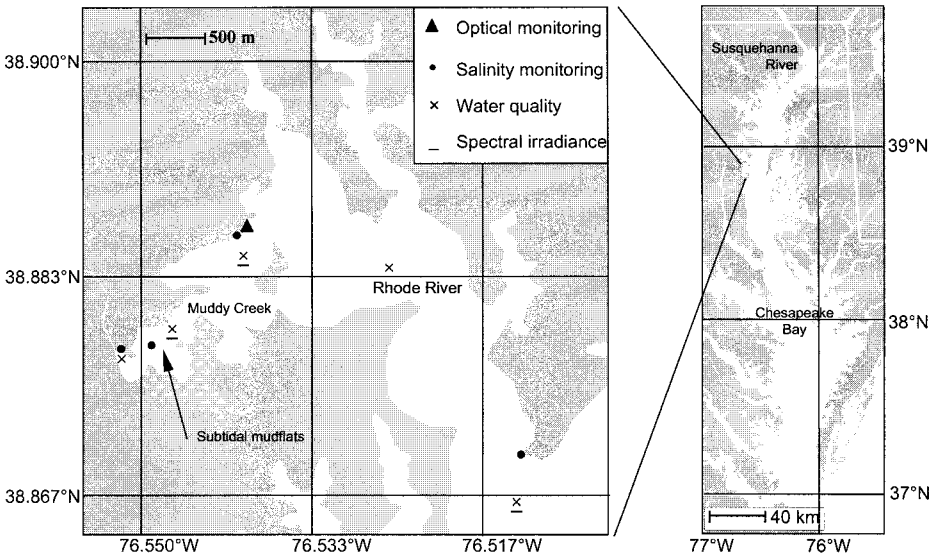

Fig. 1. Map showing the location of Rhode River, Maryland, on the western shore of Chesapeake Bay. Rhode River map shows locations of (•) automated salinity monitors, (▲) optical monitor, and (×) water quality sampling stations, three of which are also sites of spectral irradiance profiles (_).

field (Kirk 1994) as well as the emergent light field measured by remote sensing instruments (Sathyendranath and Platt 1997).

Here we use continuously monitored salinity data to document the physical processes leading to the formation of the spring 2000 bloom of *P. minimum* in the Rhode River, coupled with monitored optical properties to document bloom development and impacts on light penetration.

Materials and Methods

Study Site

The Rhode River (Maryland, U.S.) is a small tributary embayment on the western shore of the mesohaline reach of Chesapeake Bay (Fig. 1). The system is shallow (mean depth 2 m, maximum depth 4 m), turbid (Gallegos et al. 1990), and eutrophic (mean summer chlorophyll concentration = 20 to 40 mg m^{-3}, Jordan et al. 1991b; Gallegos and Jordan 1997). Salinity varies seasonally and spatially from 0 to 14 at the upstream stations and from about 2 to 20 at the mouth, depending on flow of the Susquehanna River, the main freshwater source to the upper Chesapeake Bay (Schubel and Pritchard 1986; Jordan et al. 1991a). The mean tidal range is 30 cm, but wind and barometric pressure gradients frequently cause much larger changes in water level.

Salinity Monitors

Hydrolab Minisondes equipped with temperature and specific-conductance probes and internal data loggers were placed at a depth of about 1 m at 4 locations. These sites were the mouth of the Rhode River where it joins Chesapeake Bay, the Smithsonian pier in the mouth of Muddy Creek (i.e., the principal freshwater tributary to the Rhode River, see Jordan et al. 1991a), the subtidal mudflats downstream of the divergence of Muddy Creek, and a fish weir that spans the constriction of Muddy Creek where it first widens into the subtidal mudflats (see Fig. 1, circles).

Optical Monitoring

Spectral absorption [a(λ)] and attenuation [c(λ)] coefficients were measured at 9 wavelengths, 412, 440, 488, 510, 532, 555, 650, 676, and 715 nm, using a flow-through absorption-attenuation meter (ac9, WETLabs). Three different ac9 units, 2 with 10 cm pathlength and one with 25 cm pathlength, were used in this work, and they are not distinguished from one another in analysis of the data. Flow to the ac9 was by gravity feed. Water from the estuary was pumped into an open topped polyvinyl chloride (PVC) cylinder with a return arm to provide a constant head. A spigot and tubing located near the bottom of the cylinder conducted water past a bubble trap standpipe to the ac9. A WETLabs MPak was used to control the ac9 and log the data. Once per hour the ac9 was turned on, allowed to warm up for 5 min, and sampled for 1 min at 6 hz. Corrections for the temperature and salinity dependence of the absorption coefficient of pure water were applied to the data according to the manufacturer's specifications.

The PVC cylinder, ac9, and MPak were housed in a monitoring shed at the end of the Smithsonian pier on the Rhode River (Fig. 1, triangle). To reduce fouling within the cylinder, the pump was operated only 15 min h^{-1}, extending from about 10 min before to 5 min after sampling by the ac9. At the conclusion of a sampling cycle, a solenoid valve was opened that allowed about 60 ml of bromide solution to flow through the standpipe and ac9 to inhibit growth of fouling organisms on the optical surfaces of the ac9. Timing of the pump and solenoid valve were controlled by a Campbell Scientific CR10 data logger and control module.

In Situ Samples and Measurements

Samples for phytoplankton chlorophyll and species composition were collected along a transect of 6 stations from 1.4 km downstream to 5.5 km upstream of the mouth of the Rhode River (Fig. 1, crosses). Samples for chlorophyll and species identification were collected from the Secchi depth using a Labline Teflon sampler. An additional sample for chlorophyll and nutrient concentrations was collected by slowly lowering and raising the sampler from the surface to the bottom as it filled (Gallegos et al. 1990). Vertically integrated samples give a better indicator of total water column pigment biomass whenever a subsurface peak is present (Gallegos et al. 1990). Samples were placed in a cooler on the boat and transported to the laboratory for filtration, which was generally completed within 3 h of sampling.

We measured profiles of downwelling (14 wavebands) and upwelling (7 wavebands) cosine-corrected spectral irradiance using a combination of 3 Satlantic OCI-200 modules. Wavebands (10 nm half-power) were centered at 325, 340, 380, 533, 555, 619, and 706 nm (downwelling only) and 412, 443, 490, 510, 550, 665, and 683 nm (downwelling and upwelling). Three stations were occupied, which were a subset of those occupied for water quality samples (Fig. 1, underbars).

Underwater light spectra were measured at 0.1 m intervals in the upper 0.5 m to resolve attenuation in the blue and ultraviolet wavebands, and at 0.25 to 1 m increments below that, depending on total depth. Only results for visible wavelengths are considered here. Electronic signals from the sensors were transmitted to the surface by a Satlantic Data-100 where they were logged as binary files by a laptop computer using the manufacturer's WinProView software. Signals were then converted to spectral irradiance units by the manufacturer's software and calibration files. Irradiance readings at each depth were normalized to deck readings of photosynthetically active radiation (PAR) logged simultaneously with a LICOR 192 sensor and LI-1400 logger. Spectral diffuse attenuation coefficients were calculated by regression of log transformed normalized irradiance against depth.

Vertically integrated water samples were collected in conjunction with irradiance profiles as above. Samples were transported to the laboratory for measurement of optical properties and optical water quality parameters (see below); but irradiance profiles were generally done on different days than the nutrient, chlorophyll, and species composition collections described above.

Water Quality Analyses

Subsamples for chlorophyll analyses were filtered onto Whatman GF/F glass-fiber filters immediately upon returning to the laboratory. Filters were extracted in 10 ml of 90% acetone overnight at 4°C either immediately or after freezing up to 4 wk. Frozen filters were thawed and extracted overnight at 4°C in the dark. Chlorophyll concentrations, uncorrected for phaeopigments, were calculated from spectrophotometric absorbance measurements by the equations of Jeffrey and Humphrey (1975).

Subsamples for species identification were preserved immediately in the field using 1% acid Lugol's solution and stored in 125 ml polyethylene bottles kept in the dark until counting (6 to 8 mo). For counting, 1 to 10 ml were settled (minimum 4 h) and viewed at a magnification of 512× under an inverted microscope (Gallegos 1992). Here we only report concentrations of the dominant bloom organism, *P. minimum,* as well as empty thecae of *P. minimum* as an indicator of increasing detritus toward the termination of the bloom (see Results). Organisms commonly considered members of the benthic periphyton (e.g., pennate diatoms) were never abundant in these samples.

Additional water quality data for upper Chesapeake Bay were obtained from the web site of the Chesapeake Bay Program at http://www.chesapeakebay.net/wquality.htm. The web site has a link to documents that fully describe methods of collection and sample processing.

Optical Properties

In the laboratory we measured absorption [$a(\lambda)$] and beam attenuation [$c(\lambda)$] coefficients of water sampled in conjunction with the spectral irradiance profiles using one of the ac9s. Water was gravity-fed through the instrument at a flow rate of about 1.5 liters min^{-1}, and data were logged using the manufacturer's Wetview software. Temperature- and salinity-corrected absorption coefficients were corrected for backscatter as described below (Eq. 3).

We measured absorption by CDOM on water fil-

tered through a 0.2 μm pore-diameter polycarbonate membrane filter (Poretics) using 5-cm pathlength quartz cells in a Cary dual beam spectrophotometer. Measurements in absorption units (AU) were converted to in situ absorption coefficients, $a_g(\lambda)$, by multiplying by 2.303 [i.e., ln(10)] and dividing by the pathlength, 0.05 m.

Data Analysis

Partitioning Absorption Coefficients

To determine the relative effect of the various optical water quality parameters on light absorption during the bloom, it is desirable to decompose the absorption coefficients into components due to different materials. Details of our procedure for determining the absorption due to phytoplankton, CDOM, and SPM are described elsewhere (Gallegos and Neale 2002). Here we describe only the terms that are to be estimated.

Absorption coefficient is an inherent optical property (Preisendorfer 1976) and may be expressed as the sum of contributions by individual components. Absorption measurements in the ac9 are referenced to absorption coefficients of optically pure water which are subtracted during the data processing. We may express the total absorption coefficient less that due to water, $a_{t\text{-}w}(\lambda)$, as derived from ac9 measurements as the sum of dissolved and particulate absorption,

$$a_{t-w}(\lambda) = a_g(\lambda) + a_p(\lambda) = a_g(\lambda) + a_{p-\phi}(\lambda) + a_\phi(\lambda) \quad (1)$$

where λ = wavelength, a_g is the absorption by CDOM (i.e., gilvin; Kirk 1994), and the absorption by particulate matter, $a_p(\lambda)$, is the sum of absorption by phytoplankton pigment, $a_\phi(\lambda)$, and by non-pigmented particulate matter, $a_{p-\phi}(\lambda)$. Operationally, $a_{p-\phi}(\lambda)$ includes absorption by non-pigmented cellular material of living phytoplankton and heterotrophic plankton, plant and animal detritus, and mineral particles.

We now define normalized absorption spectra for each of the components,

$$g(\lambda) = \frac{a_g(\lambda)}{a_g(440)} \quad (2a)$$

$$\phi(\lambda) = \frac{a_\phi(\lambda)}{a_\phi(676)} \quad (2b)$$

$$p(\lambda) = \frac{a_{p-\phi}(\lambda)}{a_{p-\phi}(440)} \quad (2c)$$

where $g(\lambda)$, $\phi(\lambda)$, and $p(\lambda)$ are the normalized absorption spectra for CDOM, phytoplankton pigment, and non-pigmented particulates, respectively. 440 nm was chosen as a reference wavelength for absorption by CDOM and non-pigmented particulates by convention, and 676 nm was chosen for normalizing $a_\phi(\lambda)$ because it is the location of an absorption peak for phytoplankton chlorophyll that is readily distinguished from CDOM and other particulate matter.

Absorption coefficients measured with the ac9 are overestimates of the true absorption coefficient due to incomplete collection of scattered photons in the reflective tube that estimates a (Kirk 1992). The overestimate is proportional to measured scattering coefficient by a coefficient, ϵ,

$$a_{t-w}(\lambda) = a_m(\lambda) - \epsilon[c(\lambda) - a_m(\lambda)] = a_m(\lambda) - \epsilon b_m(\lambda) \quad (3)$$

where $a_m(\lambda)$ = absorption coefficient actually measured by the ac9, and the measured scattering coefficient, $b_m(\lambda)$, is the difference between the beam attenuation coefficient, $c(\lambda)$, and $a_m(\lambda)$. The value of ϵ depends on the composition of the particulate matter and is considered to vary between 0.07 for organic particles to 0.18 for marine inorganic particulates (Kirk 1992), though we have estimated higher values, especially in samples influenced by terrestrial runoff.

Assuming that mean spectral values for the normalized absorption spectra can be determined for a region of interest, then the characteristic absorption coefficients at the appropriate reference wavelengths can be determined by solving the system,

$$\mathbf{a_0} = \mathbf{N_0}^{-1} \times \mathbf{a_m} \quad (4)$$

where $\mathbf{a_0}$ is the vector of coefficients to be estimated, $[a_g(440), a_\phi(676), a_{p-\phi}(440), \epsilon]^T$, $\mathbf{a_m}$ is the vector of absorption coefficients measured by the ac9, $[a_m(\lambda_1), \ldots, a_m(\lambda_4)]^T$, and $\mathbf{N_0}$ is the matrix of coefficients,

$$\mathbf{N}_0 = \begin{bmatrix} g(\lambda_1) & \phi(\lambda_1) & p(\lambda_1) & b_m(\lambda_1) \\ \vdots & & & \vdots \\ g(\lambda_4) & \phi(\lambda_4) & p(\lambda_4) & b_m(\lambda_4) \end{bmatrix} \quad (5)$$

If the normalized absorption spectra were invariant and perfectly known and if $a_m(\lambda)$ were error-free, the choice of wavelengths in Eq. 5 would not matter. Due to expected levels of uncertainties, we choose wavelengths to maximize the information about the unknown absorption coefficients. We routinely use λ_1 = 412 nm because it is a maximum (among the wavelengths available with the ac9) for absorption by CDOM, λ_2 = 488 nm because it is the wavelength at which $g(\lambda)$, $\phi(\lambda)$, and $p(\lambda)$ have their maximum separation, λ_3 = 676 nm because it is an absorption peak for $\phi(\lambda)$, and 715 nm because $a_m(715)$ is governed largely by ϵ. This procedure makes no assumptions regarding negligible

absorption by CDOM or by non-algal particulate matter at either 676 or 715 nm. Equations 4–5 neither require nor use any supporting measurements that may be available, though additional measurements of, e.g., $a_g(440)$, can be incorporated into the solution procedure when available to stabilize the estimates (Gallegos and Neale 2002).

Estimating Diffuse Attenuation Coefficients from a and b

Light availability decreases with depth in the water approximately according to a negative exponential,

$$E_d(z) = E_0 \exp(-K_d z) \quad (6)$$

$E_d(z)$ = downwelling, cosine-corrected irradiance at depth, z, E_0 = irradiance just below the water surface, and K_d = diffuse attenuation coefficient for downwelling irradiance. K_d is not an inherent optical property as are absorption and scattering coefficients (Kirk 1994). Using Monte Carlo modeling of the equations of radiative transfer, Kirk (1984, 1994) has established the following useful relationship between K_d and inherent optical properties,

$$K_d = \frac{1}{\mu_0}\sqrt{a_t^2 + G(\mu_0)ab} \quad (7)$$

where μ_0 = cosine (relative to the zenith) of the solar incidence angle after refraction at the air-water interface, and $G(\mu_0)$ is an empirical linear function of μ_0 that depends on angular scattering properties of the particulate matter and the optical depth in the water.

To determine the impact of the dinoflagellate bloom on light penetration we used Eq. 7 with ac9 measurements of a and b to calculate diffuse attenuation coefficients. We first tested this method of calculating $K_d(\lambda)$ by comparing calculations with profile measurements made with the Satlantic spectroradiometer at wavelengths that the 2 instruments had in common. Finding K_d calculated according to Eq. 7 to be an acceptable estimate of measured K_d (see Results), we used a and b measured by in situ monitoring in Eq. 7, holding μ_0 constant at a value calculated for 1100 local time on April 15. This enabled us to calculate $K_d(\lambda)$ even during nighttime hours when K_d technically is undefined, and thereby obtain a more complete record of bloom development than had we considered daylight hours only. We then calculated the diffuse attenuation coefficient for PAR, $K_d(PAR)$, from the calculated $K_d(\lambda)$ by interpolation and integration of the diffuse attenuation spectrum (see Gallegos 1994).

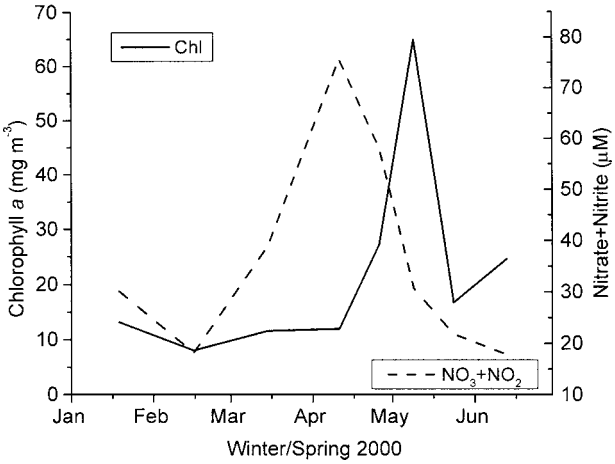

Fig. 2. Time course of nitrate + nitrite concentration (dashed line) and chlorophyll concentration (solid line) at station 3.3C on the mainstem of Chesapeake Bay at the bay bridge (39°N). Data indicate the approximate maximal concentrations of nutrients and chlorophyll that might have been imported to western shore tributaries during the spring of 2000. Data are from Chesapeake Bay Water Quality Monitoring Program.

Results

Bloom Development

The spring 2000 bloom of *P. minimum* was a widespread phenomenon in upper Chesapeake Bay. Since water renewal in the shallow western shore tributaries is driven by surface water of Chesapeake Bay (Schubel and Pritchard 1986), it is useful to first examine bloom development in the main stem of the bay. Data from the Chesapeake Bay Water Quality Monitoring Program indicate that surface concentrations of nitrate + nitrite at the Bay Bridge (39°N) rose to 70 µM in mid-March to early April, and then declined as surface chlorophyll concentrations rose to 65 mg m^{-3} in mid-April to early May (Fig. 2). Higher chlorophyll concentrations (120 mg m^{-3}) were observed in surface waters along the western shore of the mainstem of Chesapeake Bay to the south of the Rhode River at 38.81°N on May 9, 2000—well after the peak concentrations in the Rhode River (data not shown). For the purpose of this analysis, we conclude that, even though the bloom was widespread in upper Chesapeake Bay, the highest chlorophyll concentrations that were available for import into the Rhode River at the time of bloom commencement was about 65 mg m^{-3}, and this occurred in early May (Fig. 2).

Monthly samples from the Chesapeake Bay Water Quality Monitoring Program indicate steadily declining surface salinities at the Bay Bridge between February and April 2000 (Fig. 3a). Continuously monitored salinity at the mouth of the Rhode River, however, shows variability about a

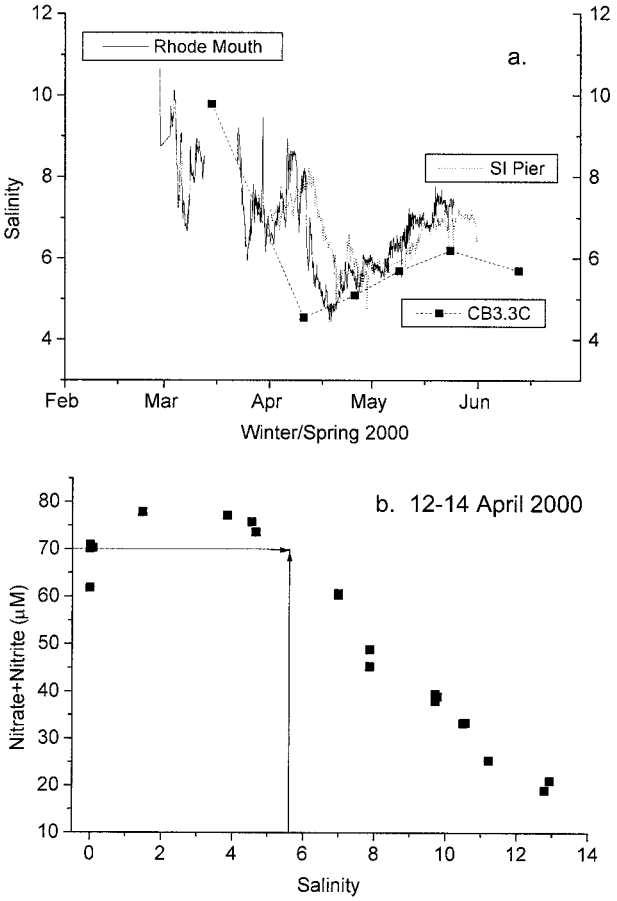

Fig. 3. (a) Time series of salinity showing intrusion of freshet into the Rhode River in mid-April 2000. Salinity was measured on bi-monthly cruises at mainstem Chesapeake Bay station 3.3C (squares) and by automated monitors at the Rhode River mouth (solid line) and Smithsonian pier (dotted line). (b) Relationship between salinity and nitrate + nitrite concentration for the mainstem of upper Chesapeake Bay during the freshet intrusion in mid-April 2000. Based on minimum salinity observed at station 3.3C (ca. 4.6), maximal concentrations of nitrate + nitrite would have been about 70 μM (arrows).

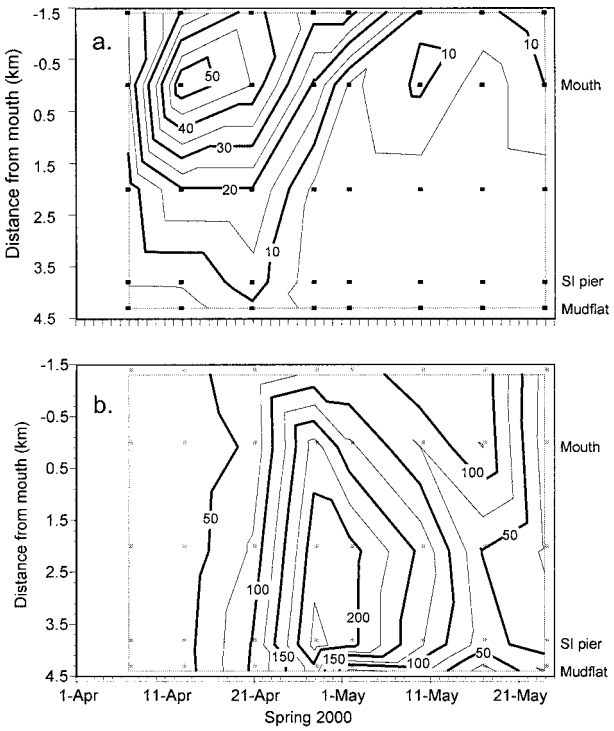

Fig. 4. (a) Contours through distance (from mouth, positive up-estuary) and time of nitrate concentration in vertically integrated samples taken on weekly cruises of the Rhode River, Maryland, in April and May 2000. Small gray squares denote sampling grid. Units of NO_3 concentration are μM. (b) Same as (a), but for chlorophyll concentration (mg m^{-3}).

gradually declining trend in March, followed by a sudden drop from 8 to 4.4 over a 7 d period from April 11 to 18. The sudden arrival of fresher water at the mouth of the Rhode River set up an inverse estuarine salinity gradient within the subestuary (Fig. 3a). Salinity at the Smithsonian pier declined rapidly in parallel with that at the mouth due to density driven circulation (Han 1974; Schubel and Pritchard 1986). The longitudinal salinity difference had dissipated by about April 21. Based on salinity-nitrate data from the Chesapeake Bay Monitoring Program taken at the time of the freshet, we estimate that nitrate concentration of water entering the Rhode River was potentially as high as 70 μM (Fig. 3b).

Most of the influx of freshwater at the mouth of the Rhode River occurred between the weekly samplings of May 13 and 21, 2000 (cf., Figs. 3a and 4a). The highest nitrate concentration observed within the Rhode River was just over 50 μM at the mouth on April 13 (Fig. 4a). Contours of nitrate concentration suggest considerable consumption during transport, because the concentration at the upper mudflat station (4.3 km) never exceeded 10 μM (Fig. 4a).

Vertically averaged chlorophyll concentrations in weekly cruise samples from the Rhode River were spatially uniform in early through mid-April (Fig. 4b). Concentrations in the first 2 sampling dates in April, which encompassed the period of density driven freshet intrusion, ranged from 28 to 44 mg m^{-3}, the highest being observed in the most bayward sample on April 13, 2000. Some evidence of spatial gradients was observed on April 21, 2000, corresponding to the time of dissipation of the longitudinal salinity gradient. The highest chlorophyll concentrations and strongest spatial gradients were observed on the next sampling on April 28, 2000, with concentrations ranging from $>$ 250 mg m^{-3} in the region near the Smithsonian dock to about 75 mg m^{-3} beyond the mouth of the Rhode River.

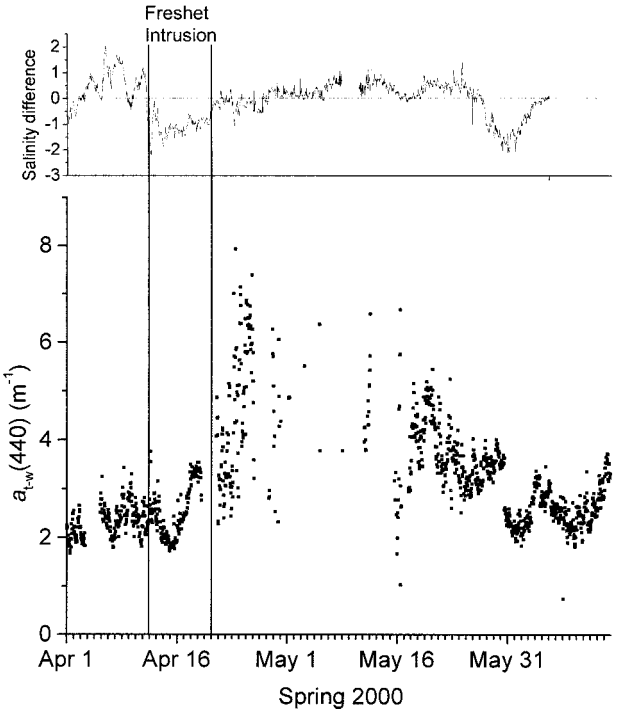

Fig. 5. Time series of absorption coefficient at 440 nm, measured by WETLabs Spectral ac9, corrected for instrument drift and backscatter error before, during, and after spring bloom of *Prorocentrum minimum,* April–May 2000. Upper panel shows the difference between monitored salinity at the mouth less that at the Smithsonian pier, which is the location of the optical monitor. Negative salinity difference indicates lower salinity at the mouth due to freshet of the Susquehanna River. Marked increase in overall magnitude of absorption coefficient and temporal variability coincides with dissipation of the longitudinal salinity distribution on April 21, 2000.

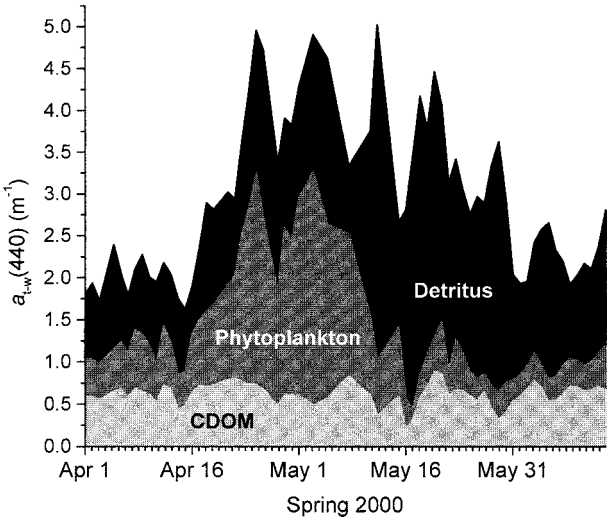

Fig. 6. Daily averages of absorption at 440 nm by the three optical components during the spring dinoflagellate bloom of 2000: colored dissolved organic matter (CDOM, light gray shading), phytoplankton pigment (dark gray shading), and non-pigmented particulate matter (detritus, black shading) estimated using Eqs. 4–5 (see text).

The bloom subsided over the next 4 weeks, so that by May 24, 2000, chlorophyll concentrations were back under 25 mg m^{-3} throughout most of the Rhode River (Fig. 4).

Optical Properties

Absorption and scattering coefficients were continuously monitored from early April through mid-June with gaps in the data especially during May due to intermittent recorder failure (Fig. 5). Absorption coefficients at 440 nm ranged from < 2 to > 7 m^{-1}. The data show a high degree of within-day variability due to tidal advection (Gallegos and Neale 2002), but some features related to the onset of the bloom can be recognized. From April 15 to 19 there was a steady rise and reduced short-term variability in $a_{t-w}(440)$, corresponding to the time period when the longitudinal inverse salinity gradient was equilibrating. Both the mean and the variability in $a_{t-w}(440)$ increased rapidly in the days following equilibration of the salinity gradient on April 21. A more gradual intrusion of freshwater into the system in late May had a similar but lesser impact on the system because it carried less nitrate and produced a smaller salinity change within the Rhode River than the freshwater intrusion in April.

Estimates of absorption at 440 nm by the three optical components were of roughly similar magnitude prior to the onset of the *Prorocentrum* bloom on April 15 (Fig. 6). Absorption by CDOM, phytoplankton, and detritus each varied between about 0.4 and 1.0 m^{-1}, so that total absorption at 440 nm varied between about 2 to 2.5 m^{-1}. During the advective phase of the bloom initiation (April 15–21, 2000) absorption by all three components rose steadily, with phytoplankton absorption rising at a slightly higher rate than the others. Phytoplankton was the predominant absorption component during the peak of the bloom from April 21 to May 9, 2000. From that point absorption by phytoplankton decreased while that by detritus increased, keeping total absorption at 440 nm near peak levels until late May and prolonging the overall optical impact of the bloom.

Various ancillary measurements taken at the water quality station closest to the Smithsonian pier support the overall magnitude of absorption attributed to the different optical components. Direct measurements of absorption by CDOM at 440 nm confirm the overall magnitude and major trends in $a_g(440)$ estimated by application of the algorithm of Gallegos and Neale (2002), with exception of a few apparent overestimates by the algorithm in mid-May (Fig. 7a). Estimated absorption

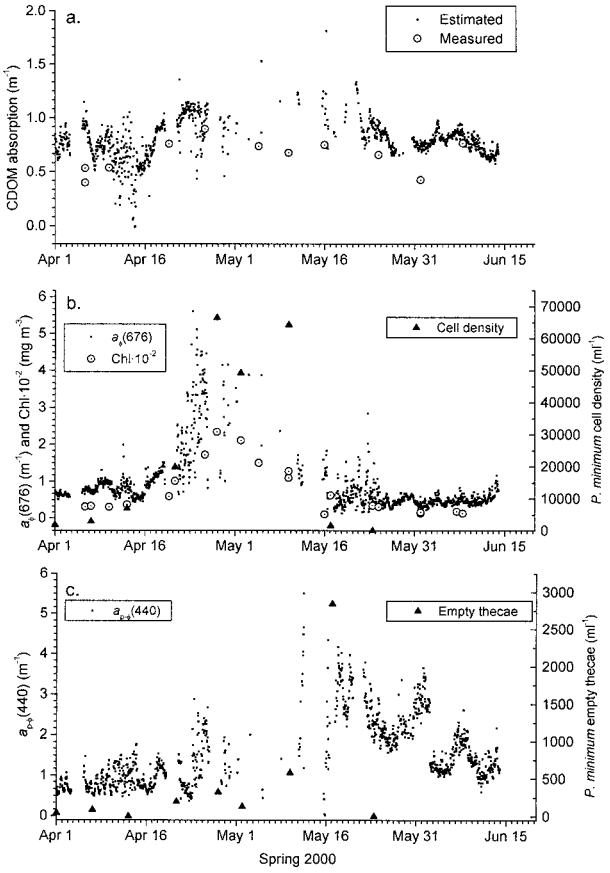

Fig. 7. Comparison of estimated components of absorption with ancillary measurements during the spring dinoflagellate bloom of 2000. (a) estimated (small solid squares) and measured absorption by CDOM, $a_g(440)$; (b) estimated absorption by phytoplankton, $a_\phi(676)$ (small solid squares), chlorophyll concentration $\times 10^{-2}$ (open circles), and cell density of *Prorocentrum minimum* (solid triangles).

by phytoplankton shows a similar trend as measurements of chlorophyll concentration and cell density of *P. minimum* (Fig. 7b), albeit peak estimates of $a_\phi(676)$ occurred in between discrete sampling events. An abrupt increase in estimated $a_{p\text{-}\phi}$ when a_ϕ declined in mid-May corresponded with a sudden increase in empty thecae of *P. minimum* between the May 10 and 17 sampling dates (Fig. 7c), as well as a sudden disappearance of live *P. minimum* cells (Fig. 7b). We suspect, therefore, that the initial increase in detrital absorption was due to cellular remains of dead *Prorocentrum* cells.

Impact of Bloom on Light Attenuation

Spectral diffuse attenuation coefficients determined in 113 profiles in the Rhode River varied from about 0.4 m^{-1} (555 nm) to 14 m^{-1} (412 and 443 nm; Fig. 8). The coefficient of determination between measured spectral diffuse attenuation coefficients and those determined according to Eq. 7 was 0.76 (0.8 on log-transformed data), and the uniform scatter using log-transformed axes (Fig. 8) indicates that the residual is approximately a constant percentage of the measured value. There was a slight tendency for values calculated by Eq. 7 to overestimate measurements (mean observed-calculated = -0.12 m^{-1}). In these waters, $K_d(555)$ tends to approximate K_d(PAR) (Gallegos 2001). It would appear that calculations of K_d(PAR) from monitored spectral absorption and scattering coefficients should give reasonable estimates of measured values (Fig. 8).

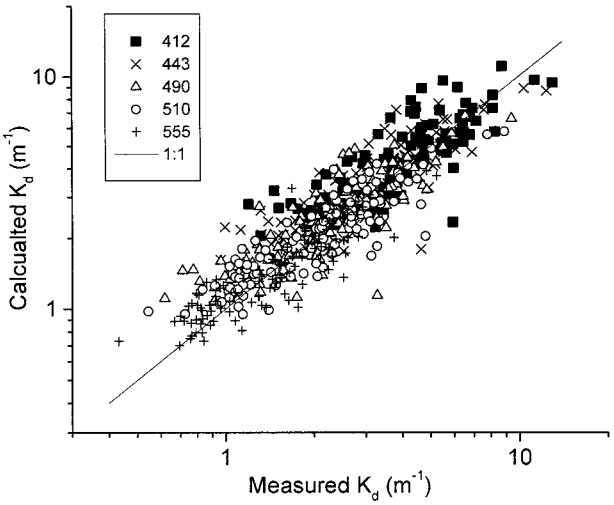

Fig. 8. Comparison of diffuse attenuation coefficients calculated by Eq. 7 using absorption and scattering coefficients measured by the WETLabs ac9 with those measured using a Satlantic spectral radiometer. Comparisons are made at wavelengths (nm) that the instruments have in common. Line of equality included for reference.

Diffuse attenuation coefficients for PAR, [i.e., K_d(PAR)], calculated from monitored $a(\lambda)$ and $b(\lambda)$ ranged from 1.2 to about 4 m^{-1} (Fig. 9). Measured K_d(PAR) were generally within the range of those calculated from the monitored optical properties during the corresponding time period. The monitored data are much more frequent and reveal considerable variability at time scales shorter than 1 wk, the interval between most of our scheduled cruises.

Based on a minimum light requirement for submersed vascular plants of 22% of surface incident irradiance (Carter et al. 2000), and adjusting for half the tidal height of 0.22 m (Koch 2001), median K_d(PAR) needs to be < 1.24 m^{-1} during the growing season (April through October) for plants to survive to a depth of 1 m mean water level. Measured values as well as the lower extremes of monitored diffuse attenuation coefficients were near that limit prior to the onset of the bloom on April

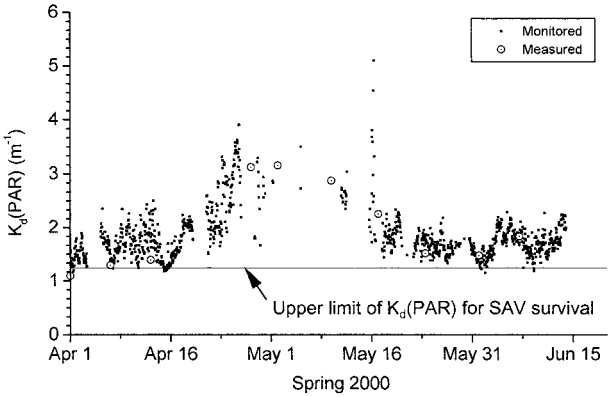

Fig. 9. Time series of diffuse attenuation coefficient for photosynthetically active radiation (PAR, 400–700 nm) calculated from monitored absorption and scattering coefficients (small solid squares) and measured in situ at a nearby station in weekly cruises (open circles) during the spring dinoflagellate bloom of 2000. Horizontal line at $K_d(PAR) = 1.24\ m^{-1}$ is the largest seasonal median attenuation coefficient (adjusted for tidal variation in the Rhode River) that would permit growth of submersed aquatic vegetation (SAV) to 1 m.

15, 2000 (Fig. 9, cf., horizontal reference line). Monitored values approach the $1.24\ m^{-1}$ limit again near the end of the bloom (ca. May 25, 2000). During the bloom both monitored and measured estimates of $K_d(PAR)$ exceed the minimum value, sometimes by as much as a factor of 3 (Fig. 9). The total duration of elevated $K_d(PAR)$ is about 40 d (April 15 to May 25). As indicated previously (Figs. 6 and 7), some of that duration is due to detritus, when *Prorocentrum* was absent from the system subsequent to May 11 (Fig. 7).

Discussion

The continuously monitored data provide a degree of resolution of the bloom development, both in terms of causative factors and system response, that cannot easily be obtained by cruise-based sampling. The spring freshet of the Susquehanna River arrived at the mouth of the Rhode River on April 11, 2000, causing a 2.1 unit drop in salinity over a 19 h period (Fig. 3a). Water exchange rates in western shore tributaries have been shown to be driven by the rate of change of salinity at the mouth (Han 1974; Schubel and Pritchard 1986). The rapid drop in salinity in early April injected nitrate into the system.

The continuously monitored optical properties helped gauge the response of the system to the nitrogen injection. The absorption components estimated from the monitored optical properties (Fig. 6) indicated that the intrusion of freshwater also carried a seed population of phytoplankton, seen as a steady rise in chlorophyll absorption from April 13–19, 2000. Local growth and formation of steep spatial gradients, indicated by increasing magnitude and short-term variance of estimated $a_\phi(676)$, commenced rapidly after the freshwater intrusion. The presence of these steep spatial gradients indicates that this isolation of nutrient rich water in the shallow zone of tributary embayments has the effect of intensifying blooms above the levels which occur in the mainstem of Chesapeake Bay. This is important for living resources of the Chesapeake Bay as a whole, because most of the area targeted for SAV restoration occurs in the highly indented shorelines of subestuaries and tributary embayments (Orth 1992).

The absence of a similar response to the freshet intrusion in late May 2000 (Fig. 5) underscores the importance of the interaction between timing and magnitude of flow events in relation to their impact on the system (e.g., Malone et al. 1996). The late May freshet was too small to deliver sufficient inorganic nitrogen to produce a bloom event in the Rhode River, even though nitrate concentration at the northern bay station was 70 μM (data from Chesapeake Bay Water Quality Monitoring Program, station CB1.1), as it was in mid-April (Fig. 3b). The high flow of the Susquehanna River in late May 1989 provides another example of the importance of freshet timing. Whereas the freshet of 1989 failed to produce the normal diatom bloom in the mainstem bay because it arrived after the seasonal shift from diatoms to flagellates (Malone et al. 1996), the late freshet did produce extraordinary blooms of dinoflagellates in western shore tributaries like the Rhode River because it was large enough to push high-nitrate water into the western mesohaline zone (Gallegos et al. 1992). The mechanism of nutrient injection followed by decreased mixing was the same as that observed here. Shallow tributary embayments are able to develop large blooms that exceed population densities in the mainstem bay because of these occasional reversals of the salinity gradients in mid- to late-spring that inject nutrients upon inversion of the normal subestuary salinity gradient, and isolate the water mass when the normal salinity gradient is being re-established.

Freshets that arrive too early in spring do not produce blooms. Gallegos and Jordan (1997) argued that high flows of the Susquehanna River in early March, as in 1993, arrive at western shore tributaries replete with nitrate, but fail to produce extraordinary blooms because they occur before sediment release rates of phosphorus are sufficient to support phytoplankton growth. It appears that under normal conditions, there is a relatively narrow window between late March and early May that spring freshets will produce extraordinary blooms of dinoflagellates. To cause a bloom, the flow must

be early enough to carry ample nitrate into the mesohaline zone, and late enough that temperature and phosphorus supply rates will support phytoplankton growth and nitrogen utilization. Measurements of nutrient release rates during 2 years in this system, which we will report elsewhere, support the contention that phosphorus release rates were insufficient to support a widespread bloom prior to mid-April.

Both the monitoring and cruise measurements indicated that diffuse attenuation coefficients in the Rhode River were too high to allow recovery of submersed grasses before and after the bloom (Fig. 9). Based on optical modeling, Gallegos (2001) calculated that long-term median concentrations of total suspended solids and chlorophyll would have to be reduced about 15% each, or chlorophyll alone by 50%, to support recovery of submersed grasses in the Rhode River. As a result of the bloom, however, attenuation coefficients were elevated above pre-bloom conditions for about 1 mo, and were approximately doubled at the peak of the bloom (Fig. 9). Moore et al. (1997) showed that a month-long turbidity pulse on the York River, Virginia, resulted in the loss of planted seagrass beds at an upriver site, without raising seasonal median concentrations of total suspended solids above levels at a down river site where planted beds survived. Scientists quoted in media reports attributed large declines of grasses in mesohaline tributaries of the Magothy, Severn, South, and Chester Rivers in 2000 to the spring bloom *P. minimum* reported here (Huslin 2001; Hyland 2001). We conclude that efforts to restore SAV must consider the effects of short-term reductions in light availability during critical growth stages.

The monitored data indicated that chlorophyll measurements alone, even when supplemented with cell counts (Fig. 7b), do not measure the full impact of blooms on light attenuation. Even though *Prorocentrum* disappeared from the system between the May 10 and May 17 sampling dates, elevated absorption by detrital matter extended the period of high attenuation coefficients into the first week of June (Fig. 7c). The appearance of high concentrations of empty thecae of *P. minimum* on May 17 suggests that dying cells from the bloom were, initially, the source of elevated detrital absorption. We suspect that such labile organic matter would not persist long, but would stimulate microbial decomposition and associated heterotrophic protists. If in fact the elevated detrital absorption was due to heterotrophic components of the community rather than suspended sediments, then management efforts to reduce these secondary impacts would have to focus on bloom prevention rather than sediment controls.

Acknowledgments

Funds for this work were provided by the Coastal Intensive Site Network (CISNet) program of the United States Environmental Protection Agency (USEPA) through grant R826943-01-0 and the Smithsonian Environmental Sciences Program. Although the research described in this article has been funded in part by the USEPA, it has not been subjected to the Agency's required peer and policy review and therefore does not necessarily reflect the views of the Agency, and no official endorsement should be inferred. We thank K. Yee and D. Sparks for assistance in the field and laboratory, and S. Hedrick for counts of phytoplankton. This paper is dedicated to the memory of Mahlon G. Kelly (Department of Environmental Sciences, University of Virginia) for his inspirational and pioneering work in the use of automated monitoring in aquatic ecology.

Literature Cited

Carter, V., N. B. Rybicki, J. M. Landwehr, and M. Naylor. 2000. Light requirements for SAV survival and growth, p. 4–15. In R. A. Batiuk, P. Bergstrom, W. M. Kemp, E. W. Koch, L. Murray, J. C. Stevenson, R. Bartleson, V. Carter, N. B. Rybicki, J. M. Landwehr, C. L. Gallegos, L. Karrh, M. Naylor, D. J. Wilcox, K. A. Moore, S. Ailstock, and M. Teichberg (eds.). Chesapeake Bay Submerged Aquatic Vegetation Water Quality and Habitat-based Requirements and Restoration Targets: A Second Technical Synthesis. U.S. Environmental Protection Agency, Chesapeake Bay Program, Annapolis, Maryland.

Chang, G. C. and T. D. Dickey. 1999. Partitioning in situ total spectral absorption by use of moored spectral absorption-attenuation meters. *Applied Optics* 38:3876–3887.

Dickey, T., D. Frye, H. Jannasch, E. Boyle, D. Manov, D. Sigurdson, J. McNeil, M. Stramska, A. Michaels, N. Nelson, D. Siegel, G. Chang, J. Wu, and A. Knap. 1998. Initial results from the Bermuda testbed mooring program. *Deep-Sea Research I* 45:771–794.

Gallegos, C. L. 1992. Photosynthesis, productivity, and species composition in a eutrophic sub-estuary: Comparison of bloom and non-bloom assemblages. *Marine Ecology Progress Series* 81: 257–267.

Gallegos, C. L. 1994. Refining habitat requirements of submersed aquatic vegetation: Role of optical models. *Estuaries* 17:198–219.

Gallegos, C. L. 2001. Calculating optical water quality targets to restore and protect submersed aquatic vegetation: Overcoming problems in partitioning the diffuse attenuation coefficient for photosynthetically active radiation. *Estuaries* 24: 381–397.

Gallegos, C. L., D. L. Correll, and J. W. Pierce. 1990. Modeling spectral diffuse attenuation, absorption, and scattering coefficients in a turbid estuary. *Limnology and Oceanography* 35: 1486–1502.

Gallegos, C. L. and T. E. Jordan. 1997. Seasonal progression of factors limiting phytoplankton pigment biomass in the Rhode River estuary, Maryland (USA). II. Modeling N versus P limitation. *Marine Ecology Progress Series* 161:199–212.

Gallegos, C. L., T. E. Jordan, and D. L. Correll. 1992. Event-scale response of phytoplankton to watershed inputs in a subestuary: Timing, magnitude, and location of phytoplankton blooms. *Limnology and Oceanography* 37:813–828.

Gallegos, C. L. and P. J. Neale. 2002. Partitioning spectral absorption in case 2 waters: Discrimination of dissolved and particulate components. *Applied Optics* 41:4220–4233.

Han, G. C. 1974. Salt balance and exchange in the Rhode River, a tributary embayment to the Chesapeake Bay. Ph.D. Dissertation, The Johns Hopkins University, Baltimore, Maryland.

Harding, L. W. J. and D. W. Coats. 1988. Photosynthetic physiology of the dinoflagellate, *Prorocentrum mariae-lebouriae,* dur-

ing its subpycnocline transport in Chesapeake Bay. *Journal of Phycology* 24:77–89.

HUSLIN, A. 2001. Bay grasses slow to gain, report says. Washington Post. May 24, 2001.

HYLAND, T. 2001. Bay grasses slipping in area rivers. The Capital Online. May 24, 2001.

JEFFREY, S. W. AND G. F. HUMPHREY. 1975. New spectrophotometric equations for determining chlorophyll *a, b, c1,* and *c2* in higher plants, algae and natural phytoplankton. *Biochemie und Physiologie der Pflanzen* 167:191–194.

JORDAN, T. E., D. L. CORRELL, J. MIKLAS, AND D. E. WELLER. 1991a. Nutrients and chlorophyll at the interface of a watershed and an estuary. *Limnology and Oceanography* 36:251–267.

JORDAN, T. E., D. L. CORRELL, J. MIKLAS, AND D. E. WELLER. 1991b. Long-term trends in estuarine nutrients and chlorophyll, and short-term effects of variation in watershed discharge. *Marine Ecology Progress Series* 75:121–132.

KELLY, M. G., G. M. HORNBERGER, AND B. J. COSBY. 1974. Continuous automated measurement of rates of photosynthesis and respiration in an undisturbed river community. *Limnology and Oceanography* 19:305–312.

KIRK, J. T. O. 1984. Dependence of relationship between apparent and inherent optical properties of water on solar altitude. *Limnology and Oceanography* 29:350–356.

KIRK, J. T. O. 1992. Monte Carlo modeling of the performance of a reflective tube absorption meter. *Applied Optics* 31:6463–6468.

KIRK, J. T. O. 1994. Light and photosynthesis in aquatic ecosystems, 2nd edition. Cambridge University Press, Cambridge, U.K.

KOCH, E. W. 2001. Beyond light: Physical, geological, and geochemical parameters as possible submersed aquatic vegetation habitat requirements. *Estuaries* 24:1–17.

MALONE, T. C., D. J. CONLEY, T. R. FISHER, P. M. GLIBERT, L. W. HARDING, AND K. G. SELLNER. 1996. Scales of nutrient-limited phytoplankton productivity in Chesapeake Bay. *Estuaries* 19: 371–385.

MOORE, K. A., R. L. WETZEL, AND R. J. ORTH. 1997. Seasonal pulses of turbidity and their relations to eelgrass (*Zostera marina* L.) survival in an estuary. *Journal of Experimental Marine Biology and Ecology* 215:115–134.

ORTH, R. J. 1992. Chesapeake Bay SAV restoration targets, p. 109–136. *In* R. A. Batiuk, R. J. Orth, K. A. Moore, W. C. Dennison, J. C. Stevenson, L. Staver, V. Carter, N. Rybicki, R. E. Hickman, S. Kollar, S. Bieber, P. Heasley, and P. Bergstrom (eds.). Submerged Aquatic Vegetation Habitat Requirements and Restoration Targets: A Technical Synthesis. Chesapeake Bay Program, U.S. Environmental Protection Agency, Annapolis, Maryland.

PREISENDORFER, R. W. 1976. Hydrologic Optics. National Oceanic and Atmospheric Administration, Washington, D.C.

RICHARDSON, K. AND B. B. JORGENSEN. 1996. Eutrophication: Definition, history and effects, p. 1–19. *In* B. B. Jorgensen and K. R. Richardson (eds.). Eutrophication in Coastal Marine Ecosystems. American Geophysical Union, Washington, D.C.

SATHYENDRANATH, S. AND T. PLATT. 1997. Analytic model of ocean color. *Applied Optics* 36:2620–2629.

SCHUBEL, J. R. AND D. W. PRITCHARD. 1986. Responses of upper Chesapeake Bay to variations in discharge of the Susquehanna River. *Estuaries* 9:236–249.

SMAYDA, T. J. 1990. Novel and nuissance phytoplankton blooms in the sea: Evidence for a global epidemic, p. 20–40. *In* E. Granéli, B. Sunderström, L. Edler, and D. M. Anderson (eds.). Toxic Marine Phytoplankton. Elsevier, New York.

TYLER, M. A. AND H. H. SELIGER. 1978. Annual subsurface transport of a red tide dinoflagellate to its bloom area: Water circulation patterns and organism distributions in the Chesapeake Bay. *Limnology and Oceanography* 23:227–246.

Received for consideration, July 30, 2001
Accepted for publication, February 4, 2002